SAKARYA UNIVERSITY
JOURNAL OF SCIENCE

e-ISSN: 2147-835X
http://www.saujs.sakarya.edu.tr

Received
22.01.2017
Accepted
10.05.2018

Doi
10.16984/saufenbilder.382220

Fe/ZnO nanorod photoanode and pyrocatechol violet sensitizer based dye sensitized solar cells

Soner Cakar[1]

Abstract

A ZnO and Fe/ZnO nanorods have been prepared and used in dye sensitized solar cells. The prepared ZnO and Fe/ZnO nanorods were characterized by XRD, SEM and SEM-EDS. Additionally, the pyrocatechol violet solutions with different pH values have been prepared, characterized and used in dye sensitized solar cells. The dyes which have different pH values were characterized via UV-Vis absorbance and cyclic voltammetry techniques. The Fe doping to ZnO nanorods increased the solar cell efficiency by 20-35%. The pyrocatechol violet dye can be binded to Fe atoms on the ZnO surface and the possible mechanism was discussed in detailed. The efficiency of best solar cell is obtained 1.39% with Fe/ZnO photoanode and pH 7.5 pyrocatechol violet dye solution.

Keywords: dye sensitized solar cells, Fe/ZnO nanorods, pyrocatechol violet, different pH.

1. INTRODUCTION

Dye sensitized solar cells (DDSCs) have been researched as one of the most promising methods for low cost power production [1]–[3]. DSSCs are composed of four main component; i) photoanode electrode, ii) sensitizers, iii) electrolyte and iv) counter electrode [4], [5]. The operation mechanism of these type solar cells is as following; the sunlight illuminates the sensitizers and it can excite the electron from HOMO to LUMO band of sensitizers. Then excited electrons are injected from sensitizer onto the semiconductor conductive band. Then, this electron moves to the counter electrode for back electron transfer. Meantime the electrolyte injects electron to HOMO band of sensitizers and this process has regenerated the electron. These processes are carried out simultaneously to provide an energy production by causing continuous electron movement in the solar cell [6]–[8]. The sensitizers are the main component of the DSSCs and researchers are making a lot of effort to reach the higher cell efficiency values. These sensitizers are divided into three main groups as following: metal complex dyes, metal free organic dyes and natural dyes [9]. The ruthenium bipyridine complexes are the most stable ones and they are reported to have higher efficiencies (up to ~12%) [10]. Recently, the transition metal complex based flavonoid type were the first time used in DSSCs for our previous study [11], [12]. These type cell show lower conversion efficiency, but it can be lead nontoxic and non-containing precious metal. Furthermore, it can be related environmental friendly. Additionally, they can be racing the metal free organic dye for the solar cell efficiency. Therefore, they are promising alternative for metal free organic dye sensitized solar cells.

[1] Sakarya Üniversitesi, Kimya Bölümü, cakarsoner@gmail.com

TiO_2 has widely used photoanode materials for DSSCs due to chemical stability, higher electron mobility, etc [13]. With similar band gap, ZnO is potential alternative photoanode materials owing to its unique ionic mobility (115-155 cm^2 V^{-1} s^{-1}) but the ZnO chemical stability is weaker than TiO_2 [11]. When the aqueous dye solution coated on ZnO surface, the ZnO can be dissolved to Zn^{2+} [4], [14]. This causes deformations on the surface of ZnO, thereby reducing the cell efficiency values.

Pyrocatechol violet has potential application for redox indicator as also known for fifty years. Recently it is applied for adsorption [15], supercapacitor [16] and sensor [17]. In this work the pyrocatechol violet is investigated for the first time as a sensitizer for solar cells. Pyrocatechol violet structure has been demostrated in Fig 1. It includes –OH and sulfite anion, which enables the adsorption of ZnO surface and complexation of Fe atoms.

In this work we prepared Fe coated ZnO photoanode to protected ZnO photoanode. In our previous works, we have demonstrated that Fe-tannin complexes have improved the cell efficiency for dye sensitized solar cell [14], [18]. In order to form strong complexes with Fe in pyrocatechol violet dyes prepared, Fe atoms have been doped into ZnO semiconductor.

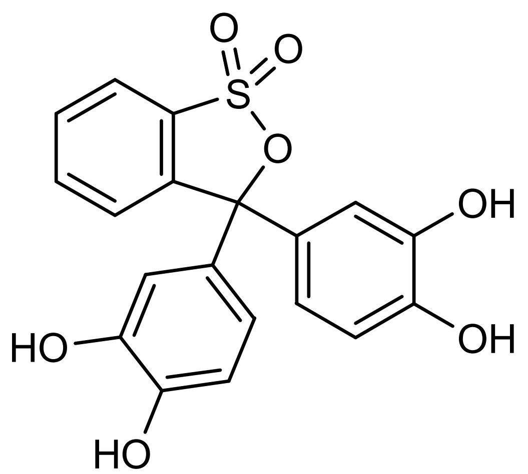

Figure 1. Pyrocatechol violet structure.

2. EXPERIMENTAL

2.1. Materials

Pyrocatechol violet ($C_{19}H_{14}O_7S$), iron (III) nitrate nonahydrate ($Fe(NO)_3.9H_2O$), zinc nitrate hexahydrate ($Zn(NO_3)_2.6H_2O$), potassium hdroxide (KOH), fluorinated tin oxide glass (FTO glass, 7 Ω/sq.), ethyl cellulose, tetrabutylammonium cis-bis(isothiocyanato) bis(2,2'-bipyridyl-4,4'-dicarboxylato) ruthenium (II) (N719 dye), 2-propanol, 4-tert butylpyridine, were purchased from Sigma Aldrich. Iodine (I_2) was obtained from Riedel de Haen. Dihydrogen hexachloroplatinate (IV) hexahydrate ($H_2PtCl_6.6H_2O$) was obtained from Alfa Aesar. All materials were analytical grade and used as received without further treatment.

2.2. Synthesis procedure of Fe/ZnO

Fe/ZnO nanostructure were synthesized via hydrothermal procedure. The detailed synthesis procedure was described in the literature [4], [14]. The amount of 4.455 g $Zn(NO_3)_2.6H_2O$ (15 mmol) and 0.217 g $Fe(NO)_3.9H_2O$ (0.5 mmol) were dissolved 60 mL ultrapure water. This solution were vigorously stirred under magnetic stirrer at 30 min. After 1.3 g KOH (23 mmol) was added to this solution and vigorously stirred at 30 min. Then this solution was transferred into the microwave hydrothermal cup (Teflon like autoclave). The microwave radiation, temperature and time are 380W, 100ºC and 1h, respectively. The mustard yellow product was centrifuged and washed with deionized water and ethanol three times. After then, The Fe/ZnO powder was dried at 60ºC for 12h. For comparison, ZnO nanoparticles were synthesized using similar procedure.

2.3. Pyrocatechol violet preparation

3.863 g (10 mM) pyrocatechol violet ($C_{19}H_{14}O_7S$) was dissolved in 50 mL deionized water. The pH of these solutions is 0.5. In the literature, the color of pyrocatechol violet is significantly dependent on pH value. The color of neutral solution (pH 0.5) is red, the solution color is changed to yellow at pH range of 2-8, and the solution color returns red-violet at higher pH values than 8. However, the basic solutions of pyrocatechol violet are unstable and lose color very quickly. This probably due to the oxidation of pyrocatechol violet. The different pH values of pyrocatechol violet solution were prepared using 0.1 M NaOH and 0.1 M HCl. The samples with different pH values were coded as following; 0.5 PCV, 3.5 PCV, 5.5 PCV, 7.5 PCV, 9.5 PCV, 11.5 PCV.

2.4. Dye sensitized solar cell assembly

The photo anode films were coated on the FTO conductive glass via doctor blade technique. The viscous paste, which includes ZnO or Fe/ZnO nanorods and ethyl cellulose were prepared and coated on FTO glass. The prepared photo anodes were sintered at 450 °C for 30 min in the air. The ZnO or Fe/ZnO photo anodes were immersed in a water solution containing 10 mM dye sensitizers for 24 h in the dark. The counter electrode was prepared by spreading out a drop of 5 mM $H_2PtCl_6.6H_2O$ solution on FTO glass and sintered at 450°C for 30 min. The electrolyte solution was a mixture of 0.05 M I_2, 0.1 M LiI and 0.5 M 4-tert-butylpyridine in acetonitrile. The photo anode and counter electrode were assembled in a typical sandwich shape and clipped together as an open cell. The internal space of these cells was filled with electrolyte solution.

2.5. Characterizations

The cyclic voltammetry (CV) measurements of pyrocatechol samples with different pH values were carried out on CHI 660C electrochemical workstation. The CV analysis were performed in a 0.1 M $LiClO_4$ solution in acetonitrile with a different scan rates by using traditional three electrode system (glassy carbon working electrode, platinum wire counter electrode and saturated calomel reference electrode). The photocurrent density-voltage curve (J-V) characteristics of the solar cells were measured by CHI 660C electrochemical workstation under 100 $mWcm^{-2}$ irradiation from a solar simulator (Xenon lamp, LCS-100, Oriel). The electrochemical impedance spectroscopy measurement (EIS) was carried out by CHI 660C electrochemical workstation in the frequency region from 0.1 Hz to 100 kHz.

3. RESULT AND DISCUSSION

3.1. Fe/ZnO characterizations

The x-ray diffraction pattern of the ZnO and Fe/ZnO nanorods are shown in Fig 2. The all diffraction peaks can be indexed in hexagonal wurtzite phase (ICDS: 98-005-7450) [4]. The peaks sharpness has demonstrate that the higher crystallinity of the ZnO phase. Because of the very small amount of doped Fe atoms was added the structure, the Fe atoms peaks was not observed in the XRD structure. However, the Fe doped into ZnO structure has changed the lattice parameters slightly. The calculated lattice parameters are listed in Table 1. The six coordinated ionic radius of Zn^{2+} and Fe^{3+} is 0.740Å and 0.645Å, respectively [19]. The ionic radius of Fe^{3+} is lower than that of Zn^{2+} and this allows the doping process possible. Additionally, the crystalline sizes of the ZnO and Fe/ZnO samples were calculated by Debye-Scherrer equations. The detailed calculation parameters were described in previous works [14], [20].

Table 1. Lattice parameters of ZnO and Fe/ZnO nanorods.

Nanorods	Lattice Parameters		Volume (Å)^3	Space Group
	a (Å)	c (Å)		
ZnO	3.251	5.210	47.65	P 63/mmc
Fe/ZnO	3.252	5.212	47.79	P 63/mmc

The mean crystalline size values of ZnO and Fe/ZnO are 120.4 and 108.7 nm, respectively. Upon Fe doping to crystalline structure, the broadening of XRD peaks is slightly increased and this results demonstrate the decreasing crystalline size.

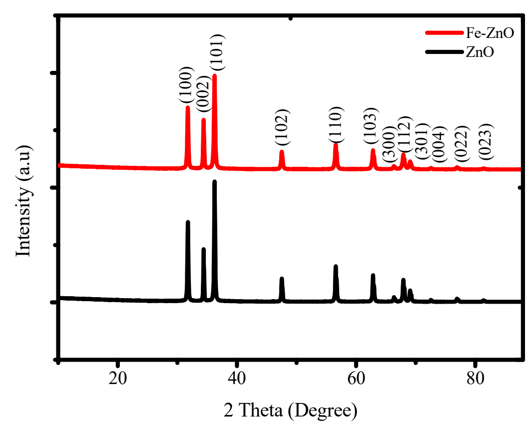

Figure 2. XRD patterns of ZnO and Fe/ZnO nanorods.

The ZnO nanorods prepared by hydrothermal methods are shown in Fig. 3A and Fe atoms doped to ZnO nanorods are shown in Fig 3B. The circles in Fig. 3B have shown the Fe atoms. The main goal of the study is to bind the Fe atoms physically to pyrocatechol violet structure. The possible binding mechanism of the Fe-pyrocatechol violet has shown in Fig 4. The –OH ion of pyrocatechol violet can bind to the Fe atoms and this can improve the dye loading capacities and also increased the cell efficiency. The FE-SEM-EDS spectra of ZnO and Fe/ZnO samples are shown in Fig 4C and D, respectively. The EDS spectrum of Fe/ZnO nanorods has shown the presence of Fe atoms.

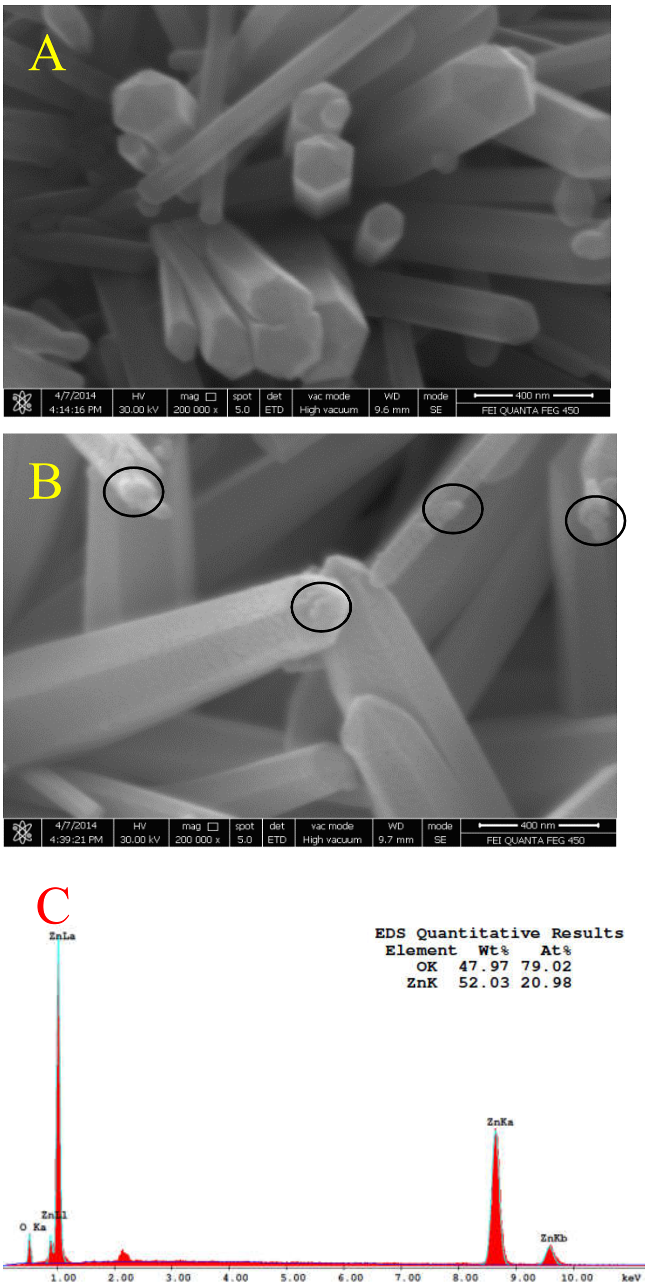

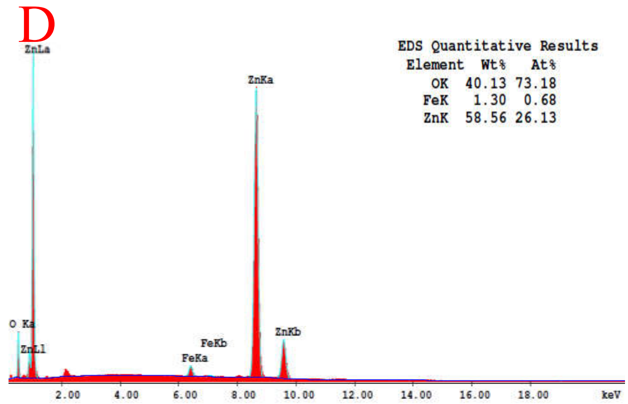

Figure 3. FE-SEM images of ZnO (A), Fe/ZnO (B) nanorods (The Fe structures were marked with a circle) and EDS spectra of ZnO (C), Fe-ZnO (C).

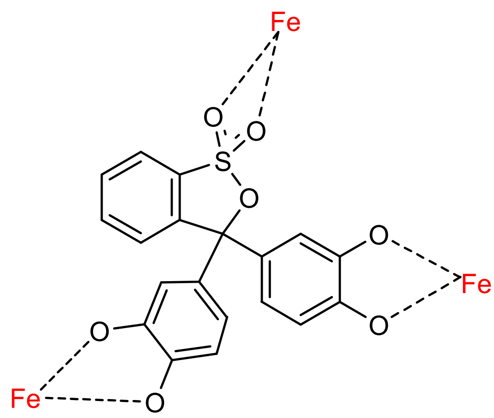

Figure 4. The possible complexation mechanism of Fe-pyrocatechol violet.

3.2. Pyrocatechol violet characterizations

The UV-Vis absorbance spectra of pyrocatechol violet different with pH values have shown in Fig 5. As can be seen in Fig. 5, the basic dye solution has also shown higher absorbance spectrum in the whole UV and VIS region compared to acidic solution. In the literature, the UV-Vis absorbance value is directly proportional to the cell efficiency values. When the dye has higher UV-Vis absorbance in the spectrum, the cell efficiency values of this type cell reach higher values. Because of this, it is predicted that the dye will have a higher cell efficiency, when it is found in the basic region. The UV-Vis absorption onset and calculated optical band gap values of these pyrocatechol violet dye solution with different pH values are summarized in Table 2.

The cyclic voltammetry of pyrocatechol violet with different pH values are shown in Fig 6. The oxidation and reduction potential of all prepared pyrocatechol dyes with different pH values are listed in Table 2 and calculation details were reported previous works [4], [21], [22].

As can be seen in Table 2 and Fig 5, the oxidation value decreased with increasing pH values. This is probably due to the fact that the increasing pH value leads to the transformation of –OH group to the =O group. Likewise, the potential for reduction has been also affected. The increasing pH has changed the oxidation and reduction potential values. This also affects the electrochemical band gap values. The optical band gap values are slightly changed with pH alteration. The optical band gap values are very similar because the optical spectra has slightly changed with the pH alteration. For this reason, the electrochemical band gap value can be used more effectively.

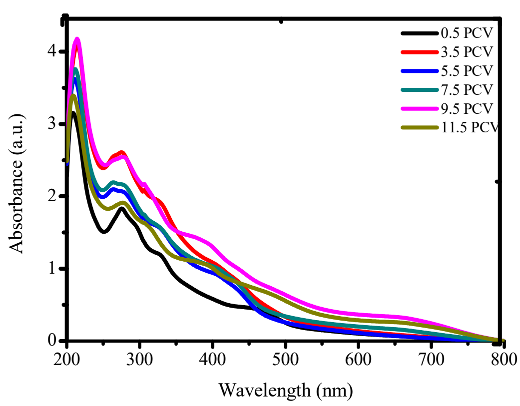

Figure 5. The UV-Vis spectra of Fe-pyrocatechol violet complex with different pH values.

Table 2. Electrochemical and optical properties of pyrocatechol violet with different pH values.

pH	UV-Vis		CV (V vs Ag/AgCl)		
	λ_{onset}	E_g^{OPT}	E_{OX}	E_{RED}	E_g^{EC}
0.5	718	1.72	-0.79	0.73	1.52
3.5	722	1.71	-0.63	0.68	1.31
5.5	725	1.70	-0.65	0.67	1.32
7.5	728	1.69	-0.44	0.58	1.02
9.5	741	1.67	-0.35	0.43	0.78
11.5	772	1.60	-0.28	0.37	0.65

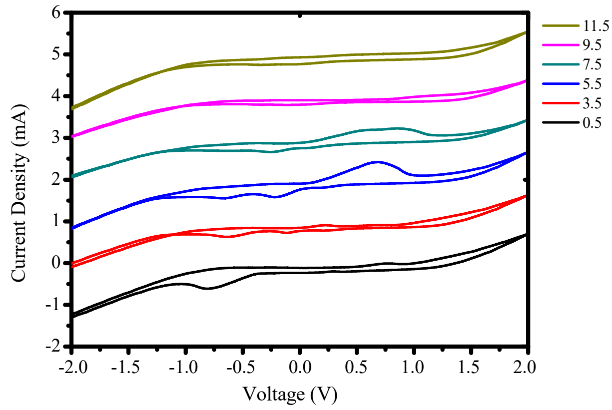

Figure 6. Cyclic voltammetry curves of pyrocatechol violet solution with different pH values.

3.3. Solar cell characterizations

The pyrocatechol violet dye based ZnO or Fe/ZnO solar cells with different pH values were investigated and current density-voltage (J-V) curves have been shown in Fig 7A and B and the photovoltaic parameters are listed in Table 3. The best solar cell is Fe/ZnO and pyrocatechol violet

Table 3. Photovoltaic parameters of ZnO and Fe/ZnO samples

	pH	Dye loading (10^{-8}mol/cm^2)	Jsc (mA/cm^2)	Voc (V)	FF (%)	η (%)
ZnO	0.5	2.81	0.72	0.85	0.47	0.29
	3.5	3.11	0.86	0.84	0.48	0.35
	5.5	4.06	1.01	0.83	0.52	0.44
	7.5	4.25	2.13	0.85	0.53	0.96
	9.5	4.44	1.55	0.82	0.50	0.63
	11.5	3.28	0.62	0.84	0.44	0.23
Fe/ZnO	0.5	3.10	1.07	0.82	0.45	0.39
	3.5	3.29	1.28	0.83	0.44	0.47
	5.5	4.24	1.52	0.85	0.51	0.66
	7.5	4.86	3.19	0.84	0.52	1.39
	9.5	5.09	2.33	0.83	0.50	0.97
	11.5	3.71	0.93	0.85	0.47	0.37

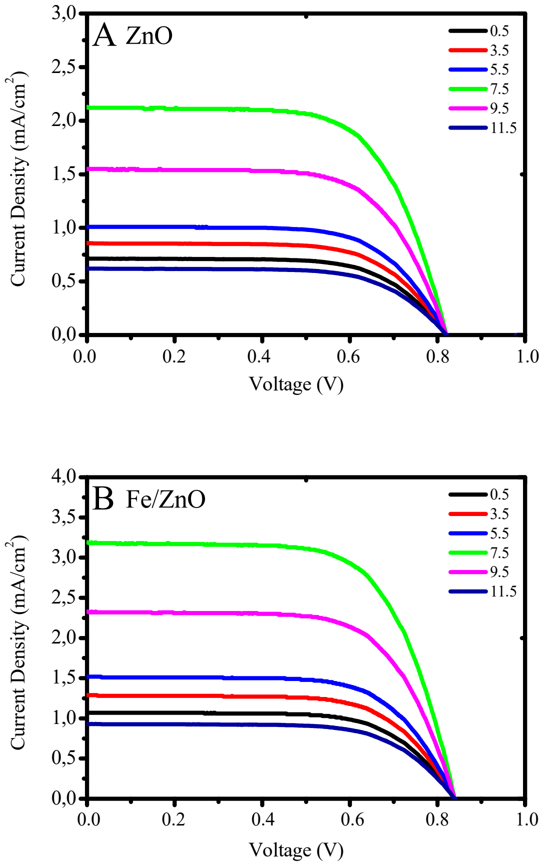

Figure 7. Current density-voltage curves of ZnO (A) and Fe/ZnO (B) samples.

solution at pH 7.5, and has a cell efficiency of 1.39 %. The solar cell efficiency values have increased after the Fe atoms addition to ZnO samples. Additionally, the solar cell efficiency values have slightly increased with the increasing pH values. However, in the basic condition (pH 9.5 and 11.5), the values have decreased. This is probably due to the fact that, in the basic condition, the dye molecules leak into solution, and in acidic condition, the ZnO or Fe/ZnO can dissolve into the solution. Due to these two shortcomings, the highest cell efficiency was observed under neutral conditions.

4. CONCLUSION

The ZnO and Fe/ZnO nanorod structures were synthesized by hydrothermal methods and characterized via XRD, FE-SEM and SEM-EDS. The pyrocatechol violet with different pH values were prepared and characterized by UV-Vis and CV technique. Then the dye sensitized solar cells was fabricated using ZnO or Fe/ZnO and pyrocatechol violet with different pH values dyes. The efficiency of best solar cell was found to be 1.39% with Fe/ZnO photoanode and pH 7.5 pyrocatechol violet dye solution. The Fe/ZnO nanorods has exhibit higher efficiencies than ZnO nanorods. These findings have confirmed that the doped Fe atoms can bind to pyrocatechol violet. The detailed complexation mechanism have been discussed. The Fe doping to ZnO nanorods have increased the dye sensitized solar cell efficiency values up to %20-35 for pyrocatechol violet with different pH dyes.

ACKNOWLEDGMENTS

This study is supported by Sakarya University Scientific Research Projects Coordination Unit. Project Number: 2016-50-02-009. I also would like to thank to Mr. Bekir Cakiroglu for his valuable contributions.

REFERENCES

A sample references list is given below;

[1] A. Hagfeldt, G. Boschloo, L. Sun, L. Kloo, and H. Pettersson, “Dye-sensitized solar cells.,” *Chem. Rev.*, vol. 110, pp. 6595–6663, 2010.

[2] N. Kannan and D. Vakeesan, “Solar energy for future world: - A review,” *Renew. Sustain. Energy Rev.*, vol. 62, pp. 1092–1105, 2016.

[3] V. Sugathan, E. John, and K. Sudhakar, “Recent improvements in dye sensitized solar cells : A review,” *Renew. Sustain. Energy Rev.*, vol. 52, pp. 54–64, 2015.

[4] S. Çakar and M. Özacar, “Fe-quercetin coupled different shaped ZnO rods based dye sensitized solar cell applications,” *Sol. Energy*, vol. 155, pp. 233–245, 2017.

[5] G. Calogero and G. Di Marco, “Red Sicilian orange and purple eggplant fruits as natural sensitizers for dye-sensitized solar cells,” *Sol. Energy Mater. Sol. Cells*, vol. 92, no. 11, pp. 1341–1346, 2008.

[6] G. Calogero, J.-H. Yum, A. Sinopoli, G. Di Marco, M. Grätzel, and M. K. Nazeeruddin, “Anthocyanins and betalains as light-harvesting pigments for dye-sensitized solar cells,” *Sol. Energy*, vol. 86, no. 5, pp. 1563–1575, May 2012.

[7] G. Calogero, A. Bartolotta, G. Di Marco, A. Di Carlo, and F. Bonaccorso, “Vegetable-based dye-sensitized solar cells,” *Chem. Soc. Rev.*, vol. 44, no. 10, pp. 3244–3294,

2015.

[8] J. Gong, J. Liang, and K. Sumathy, "Review on dye-sensitized solar cells (DSSCs): Fundamental concepts and novel materials," *Renew. Sustain. Energy Rev.*, vol. 16, no. 8, pp. 5848–5860, 2012.

[9] M. R. Narayan, "Review : Dye sensitized solar cells based on natural photosensitizers," *Renew. Sustain. Energy Rev.*, vol. 16, no. 1, pp. 208–215, 2012.

[10] J. Gong, K. Sumathy, Q. Qiao, and Z. Zhou, "Review on dye-sensitized solar cells (DSSCs): Advanced techniques and research trends," *Renew. Sustain. Energy Rev.*, vol. 68, no. December 2015, pp. 234–246, 2017.

[11] R. Vittal and K.-C. Ho, "Zinc oxide based dye-sensitized solar cells: A review," *Renew. Sustain. Energy Rev.*, 2016.

[12] H. Ejima, J. J. Richardson, and F. Caruso, "Metal-phenolic networks as a versatile platform to engineer nanomaterials and biointerfaces," *Nano Today*, vol. 12, pp. 136–148, 2016.

[13] B. Roose, S. Pathak, and U. Steiner, "Doping of TiO2 for sensitized solar cells," *Chem. Soc. Rev.*, vol. 44, no. 22, pp. 8326–8349, 2015.

[14] S. Çakar and M. Özacar, "Fe–tannic acid complex dye as photo sensitizer for different morphological ZnO based DSSCs," *Spectrochim. Acta Part A Mol. Biomol. Spectrosc.*, vol. 163, pp. 79–88, 2016.

[15] X. Wang, S. Bi, N. Gan, and Z. Wei, "Aluminum Speciation with Adsorptive Pyrocatechol Violet-Al(III) Complex by Derivative Adsorption Chronopotentiometry," *Electroanalysis*, vol. 13, no. 15, pp. 1279–1286, 2001.

[16] Q. Wang, Y. F. Nie, X. Y. Chen, Z. H. Xiao, and Z. J. Zhang, "Use of pyrocatechol violet as an effective redox additive for highly promoting the supercapacitor performances," *J. Power Sources*, vol. 323, pp. 8–16, 2016.

[17] S. Ayaz and Y. Dilgin, "Flow injection amperometric determination of hydrazine based on its electrocatalytic oxidation at pyrocatechol violet modified pencil graphite electrode," *Electrochim. Acta*, vol. 258, pp. 1086–1095, 2017.

[18] S. Çakar, N. Güy, M. Özacar, and F. Fındık, "Investigation of Vegetable Tannins and Their Iron Complex Dyes for Dye Sensitized Solar Cell Applications," *Electrochim. Acta*, vol. 209, pp. 407–422, Aug. 2016.

[19] R. D. Shannon, "Revised Effective Ionic Radii and Systematic Studies of Interatomic Distances in Halides and Chalcogenides," *Acta Crystallogr.*, vol. A32, pp. 751–767, 1976.

[20] M. R. Parra and F. Z. Haque, "Aqueous chemical route synthesis and the effect of calcination temperature on the structural and optical properties of ZnO nanoparticles," *J. Mater. Res. Technol.*, vol. 3, no. 4, pp. 363–369, Oct. 2014.

[21] J. Liu *et al.*, "New D-π-A system dye based on dithienosilole and carbazole: Synthesis, photo-electrochemical properties and dye-sensitized solar cell performance," *J. Photochem. Photobiol. A Chem.*, vol. 294, pp. 54–61, 2014.

[22] M. Han, X. Zhang, X. Zhang, C. Liao, B. Zhu, and Q. Li, "Azo-coupled zinc phthalocyanines: Towards broad absorption and application in dye-sensitized solar cells," *Polyhedron*, vol. 85, pp. 864–873, 2015.